The Astrophysical Journal, 690:L110–L113, 2009 January 10 doi:10.1088/0004-637X/690/2/L110

DETECTION OF WATER ICE GRAINS ON THE SURFACE OF THE CIRCUMSTELLAR DISK AROUND HD 142527*

M. Honda[1], A. K. Inoue[2], M. Fukagawa[3], A. Oka[4], T. Nakamoto[4], M. Ishii[5], H. Terada[5], N. Takato[5], H. Kawakita[6], Y. K. Okamoto[7], H. Shibai[3], M. Tamura[8], T. Kudo[8], and Y. Itoh[9]

[1] Department of Information Science, Kanagawa University, 2946 Tsuchiya, Hiratsuka, Kanagawa 259-1293, Japan; hondamt@kanagawa-u.ac.jp
[2] College of General Education, Osaka Sangyo University, 3-1-1, Nakagaito, Daito, Osaka 574-8530, Japan
[3] Department of Earth and Space Science, Graduate School of Science, Osaka University, 1-1 Machikaneyama, Toyonaka, Osaka 560-0043, Japan
[4] Department of Earth and Planetary Science, Tokyo Institute of Technology, Ookayama, Meguro, Tokyo 152-8551, Japan
[5] Subaru Telescope, National Astronomical Observatory of Japan, 650 North A'ohoku Place, Hilo, HI 96720, USA
[6] Department of Physics, Kyoto Sangyo University, Motoyama, Kamogamo, Kita-ku, Kyoto 603-8555, Japan
[7] Institute of Astrophysics and Planetary Sciences, Ibaraki University, 2-1-1 Bunkyo, Mito, Ibaraki 310-8512, Japan
[8] National Astronomical Observatory of Japan, 2-21-1 Osawa, Mitaka, Tokyo 181-8588, Japan
[9] Graduate School of Science, Kobe University, 1-1 Rokkodai, Kobe, Hyogo 657-8501, Japan
Received 2008 July 31; accepted 2008 November 18; published 2008 December 19

ABSTRACT

Coronagraphic imaging for the Herbig Ae star, HD 142527, was performed using the Coronagraphic Imager with Adaptive Optics (CIAO) on the 8.2 m Subaru Telescope. The images were obtained in the H_2O ice filter ($\lambda = 3.08\,\mu$m) using adaptive optics (AO), and in the L' band without AO. Combining these data with previous observational results in the H and K bands, we derived the spectra of the scattered light from the circumstellar disk around HD 142527 and detected an H_2O ice absorption feature in the spectra. This result can be explained by the presence of silicate and H_2O ice grains of $\sim 1\,\mu$m in size, according to the prediction model by Inoue et al. This grain size is consistent with previous observational study by Fukagawa et al. and Fujiwara et al. The present result demonstrates that high-resolution imaging of disk-scattered light in the ice band is useful for detecting H_2O ice grain distributions in circumstellar disks.

Key words: circumstellar matter – stars: pre-main sequence

1. INTRODUCTION

Water ice grains theoretically play a number of important roles in protoplanetary and debris disks. Ice enhances the solid material in the cold outer part of a protoplanetary disk, which promotes the formation of cores of gaseous planets (e.g., Hayashi et al. 1985). Sublimation of ice grains would form a dust ring in a debris disk (Kobayashi et al. 2008). Furthermore, icy planetesimals or comets may bring water to the Earth (e.g., Morbidelli et al. 2000). Nevertheless, observational evidence for the presence of water ice *in protoplanetary disks* and its spatial distribution has been very limited. Recently, however, water vapor has been detected in protoplanetary disks with *Spitzer Space Telescope* (e.g., Carr & Najita 2008; Salyk et al. 2008), but the detection of water ice remains elusive. Crystalline H_2O ice emission features at 44 and 62 μm have been found for a few Herbig Ae/Be stars (Malfait et al. 1999; Meeus et al. 2001), but the spatial distribution of ice is very difficult to obtain in far-infrared (FIR) because of the lack of angular resolution. While near-infrared (NIR) absorption due to water ice has been reported (Pontoppidan et al. 2005; Terada et al. 2007), a spectroscopic approach is feasible only for edge-on disks, and the radial distribution of the ice cannot be measured.

Inoue et al. (2008) have proposed a new observational method to investigate the radial distribution of ice in face-on disks. They show that ice absorption can also be found in the light scattered by icy grains and that multi-wavelength imaging in NIR wavebands, including in the H_2O band at 3.1 μm, is a useful tool to constrain the ice distribution in the disk. We have applied this method to the circumstellar disk around a Herbig Ae star, HD 142527 (F6 IIIe; Waelkens et al. 1996), which is an ideal target for imaging in the H_2O band for a number of reasons. First, its bright extended disk has already been resolved (Fukagawa et al. 2006; Fujiwara et al. 2006; Ohashi 2008). Second, it is one of only a few Herbig Ae/Be stars that show clear evidence for H_2O ice grains in FIR (Malfait et al. 1999). Although there are some different estimates regarding the distance and stellar luminosity of HD 142527 in the literature, we follow Acke & van den Ancker (2004) and use the distance of 145 pc and the stellar luminosity of 15 $L_\odot$.

In this Letter, we report the detection of H_2O ice grains in the disk around HD 142527 using multi-wavelength imaging in NIR. The result demonstrates that this observational method is useful for revealing ice distributions in protoplanetary disks.

2. OBSERVATIONS AND DATA REDUCTION

Coronagraphic imaging observations for the Herbig Ae star HD 142527 using a narrow-band H_2O ice filter (wavelength of isophotal frequency, $\lambda_{\nu_{\rm iso}} = 3.08\,\mu$m, and width $\Delta\lambda = 0.14\,\mu$m) were performed using the Coronagraphic Imager with Adaptive Optics (CIAO; Tamura et al. 2000) on the Subaru Telescope on 2007 July 26. We used the occulting masks with diameters of 0.″4 and 0.″6, but the images taken with the 0.″6 mask, in particular, have been used for later discussion. A full width at half-maximum (FWHM) of 0.″10 was achieved using the AO36. The exposure times were 3 and 5 s for each data frame with the 0.″4 and 0.″6 mask, and the total exposure times were 468 and 180 s , respectively. As a point-spread function (PSF) reference star, we observed HD 138395 after HD 142527. BS 4689 was observed as a photometric standard star. The mean flux density for BS 4689 at 3.08 μm was estimated by scaling the Kurucz's stellar model atmosphere ($T_{\rm eff} = 8800$ K, $\log g = 4.0$, solar

* Based on data collected at Subaru Telescope, which is operated by the National Astronomical Observatory of Japan.

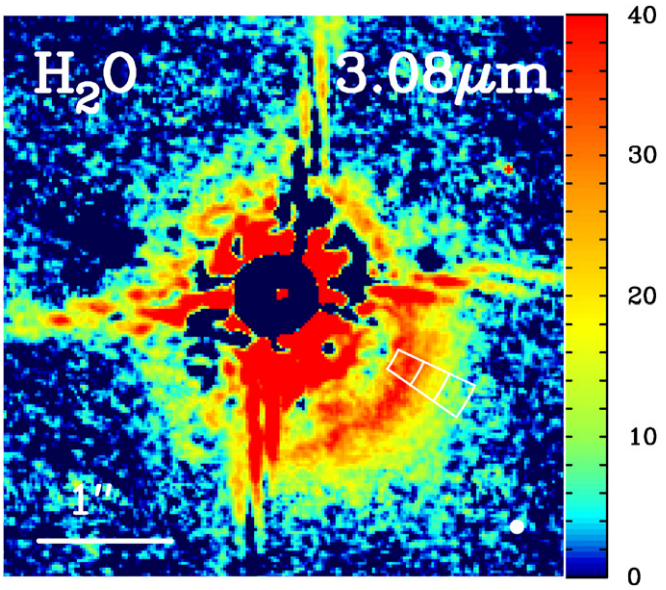

Figure 1. PSF-subtracted 3.08 μm image of the disk around HD 142527. The unit of intensity is mJy arcsec^{-2}. North is up; east is to the left. The occulting mask is 0.″6. The spatial resolution is 0.″10. The three enclosed regions (regions A, B, and C from inner to outer regions) on the southwest structure are the positions from which the spectra shown in Figure 3 are extracted.

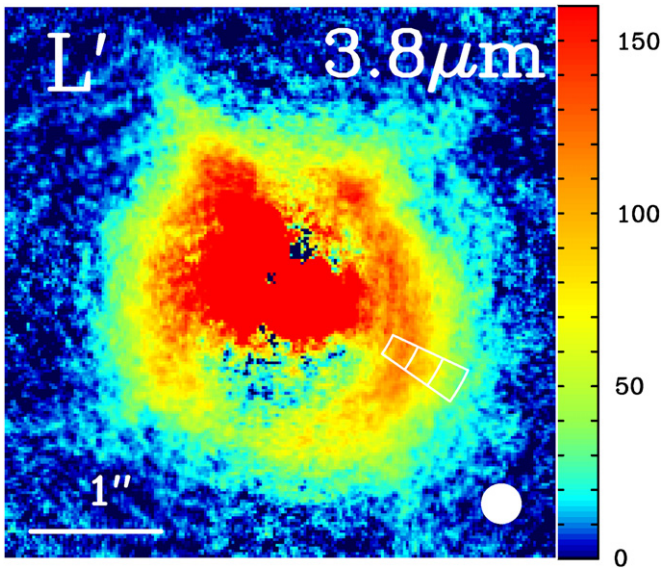

Figure 2. Same as Figure 1 but in the L' band. No occulting mask was used. The spatial resolution was 0.″3. Note that the strong emission in the northeastern direction in the L' band is an artifact of the PSF mismatch between HD 142527 and the PSF reference star.

metallicity) to match the flux density in the K and L' bands (Henden 2002; Tokunaga & Vacca 2005). The calculated flux density was 11.0 Jy at 3.08 μm.

The images obtained in the H_2O ice filter were first processed using the IRAF packages for dark subtraction, flat-fielding with sky flats, bad pixel correction, and sky subtraction. Since the stellar halo was very bright, PSF subtraction was required to investigate the structure near the central star. The reference PSF was chosen to match the PSF of HD 142527 for each frame with careful visual inspection to determine whether the circular bright halo of the central point source was well suppressed after PSF subtraction. During this analysis, each reference PSF frame was rotated to match the direction of the spider pattern of the object, then shifted and scaled to minimize the residual of the stellar halo after PSF subtraction. In order to estimate the systematic uncertainty of the surface brightness due to the PSF subtraction process, we changed the scaling of the PSF before subtraction, and measured the acceptable range of the scaling factor. The systematic uncertainty of the surface brightness was measured to be 17–25% depending on the position. This systematic uncertainty was typically larger than the statistical error derived from the standard deviation of the best PSF-subtracted object frames.

The L' band images were obtained on 2005 June 30 with CIAO. The AO36 was not available at the time, but our imaging was conducted under decent seeing conditions (better than 0.″5 at optical). Since the star was unsaturated, a coronagraphic mask was not used. For HD 142527, 50 exposures of 0.1 s were co-added into one data frame, and 58 frames were taken in total. HD 142695 was also observed as a PSF reference star just before the imaging of HD 142527. We obtained 26 frames each with the same exposure times as HD 142527. Nodding at 10″ was performed for both stars, to satisfactorily subtract the background sky. The FWHM in the L' band was 0.″3 on average for both HD 142527 and HD 142695. We observed HD 161903 as a photometric calibrator (Leggett et al. 2003). The L' band images were reduced in the same way as described by Fukagawa et al. (2006). The seven frames for HD 142527 were removed due to the large FWHMs, and the remaining 51 images were combined after subtracting the reference PSF. The inner region with 0.″8 radius was affected by the PSF-subtraction residuals and hence was photometrically unusable.

3. RESULTS

Figures 1 and 2 show the PSF-subtracted images of the circumstellar disk around HD 142527 in the H_2O ice filter (3.08 μm) with the 0.″6 mask and in the L' band (3.77 μm) without a mask, respectively. Note that the strong emission in the northeastern direction in the L' band is an artifact of the PSF mismatch between HD 142527 and the PSF reference star. The eastern and western arcs discovered by Fukagawa et al. (2006) in the H and K bands were also detected in the H_2O and L' bands. The outer spiral arm observed in the H and K bands was not detected due to the faintness of the scattered light and a lower sensitivity at the longer wavelengths.

We constructed the spectra of the disk-scattered light using images of the H, K, H_2O, and L' bands. No variability in NIR for HD 142527 was assumed, but note that the possibility of temporal change could not be ruled out. The spectra were extracted from the three regions and are shown in Figure 3: region A (0.″96 $\leqslant r <$ 1.″17, 235 $\leqslant$ P.A. $\leqslant$ 245), region B (1.″17 $\leqslant r <$ 1.″38, 235 $\leqslant$ P.A. $\leqslant$ 245), and region C (1.″38 $\leqslant r <$ 1.″60, 235 $\leqslant$ P.A. $\leqslant$ 245). The spatial resolutions in the H, K, and H_2O bands were degraded to match those in the L' band (FWHM = 0.″3) by convolving Gaussian. The spectrum for the total flux densities is also presented for comparison in the top panel of Figure 3, which shows few or no features in the H_2O band. The contribution from the scattered light to the total flux density in the H and K bands is estimated to be 3.1–3.2% (Fukagawa et al. 2006), indicating that most of the flux density in the total spectrum is attributed to the emission from the star itself and thermal emission from hot grains in the vicinity of the star where icy grains cannot survive. Therefore, the absence of a 3 μm ice feature is a natural consequence. In

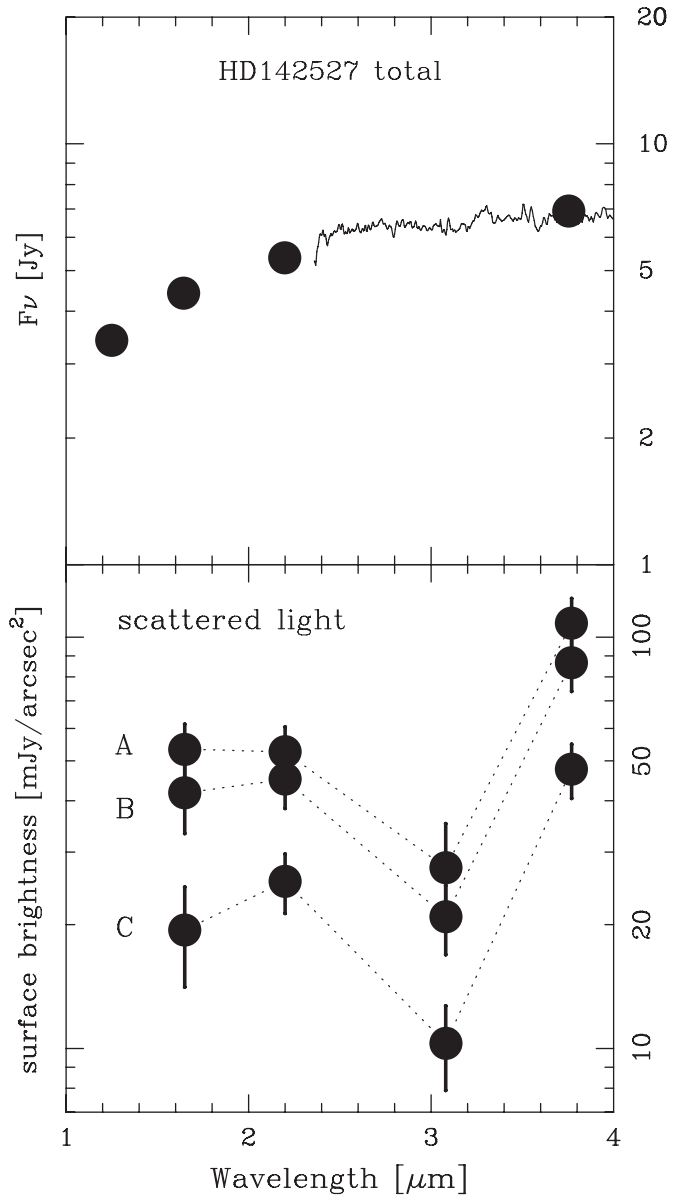

Figure 3. Top panel shows NIR photometry and a spectrum of the entire HD 142527 system, which is used as the representative of the illuminating source spectrum. Photometric values are taken from Malfait et al. (1998), and the solid line is the *ISO*/*SWS* spectrum taken from Meeus et al. (2001). The bottom panel represents the spectra of the scattered light from regions A, B, and C shown in Figure 1. By comparing the systematic and statistical errors, we used the larger one for the total error plotted in this figure. The dip in 3 μm, probably due to H_2O ice grains, is present in all the scattered light spectra, while it is not seen in the total spectrum, which is dominated by thermal emission from hot dust near the central star.

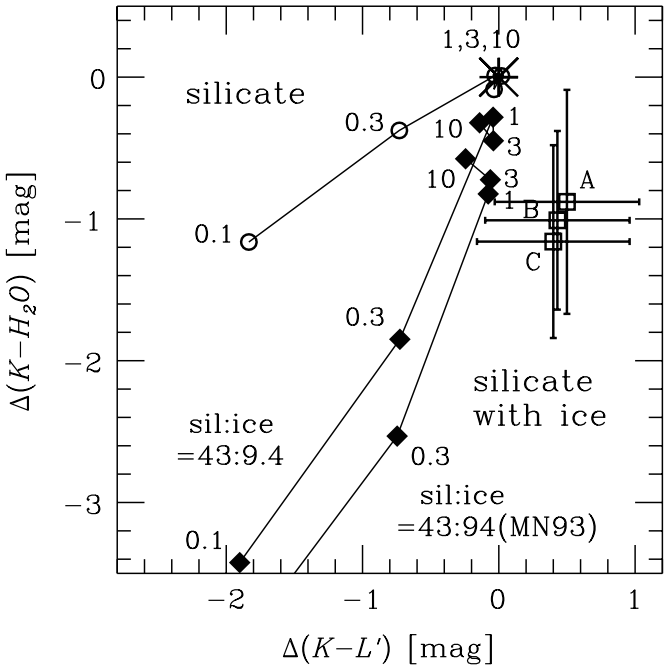

Figure 4. Two-color difference ($\Delta(K - L'$) and $\Delta(K - H_2O)$) diagram of the scattered light. Note that the origin (big asterisk) represents the position of the color of the illuminating source. The circles and diamonds are the theoretical color difference of the scattered light from the optically thick disk with silicate and silicate with ice grains, respectively (Inoue et al. 2008). Each line is the sequence of grain size: 0.1, 0.3, 1, 3, and 10 μm. Two lines of silicate with ice grains represent two different ice abundances. One is the mass abundance used by Miyake & Nakagawa (1993), and the other is the same but with a 1/10 ice abundance. The squares represent the observed color difference of regions A – C. Silicate and ice grains of $\sim 1\,\mu$m may explain the observed color difference of the scattered light, indicating the presence of H_2O ice grains on the surface of the HD 142527 disk.

contrast, the spectra of the scattered light show a clear reduction in the H_2O ice band (3.08 μm), suggesting the presence of a 3 μm absorption feature. This result can be explained by the water ice grains in the disk surface where the light scattering occurs. The presence of water ice grains is consistent with the detection of emission features at 44 and 62 μm in the FIR spectrum for HD 142527 (Malfait et al. 1999). Furthermore, Fujiwara et al. (2006) derived the dust temperature of the western disk to be around 85 ± 3 K. Since mid-infrared (MIR) emitting dust should be located in the inner region of the outer disk, the temperature of the outer surface should be lower and cold enough for water ice grains to exist. In addition to the water ice grains, the presence of hydrous silicate (montmorillonite) in HD 142527 was claimed by Malfait et al. (1999). The possibility of hydrous silicate grains contributing to the H_2O band flux reduction cannot be excluded. However, hydrous silicate grains are not the principal dust components of the HD 142527 disk (Malfait et al. 1999), and neither are other forms of ice (Whittet 2003; Davis 2007; Encrenaz 2008). Therefore, water ice is most likely the dominant carrier of the observed absorption feature.

In order to discuss the properties of scattering grains in more detail, we compared our results with the model predictions by Inoue et al. (2008) using a color difference diagram ($\Delta(K - H_2O)$ versus $\Delta(K - L')$). The color of the scattered light depends on the color of the illuminating source. Since the fraction of the scattered light to the total flux is very small (Fukagawa et al. 2006), we assume that the total flux represents the illuminating source. The mean flux density for the entire HD 142527 system within the H_2O band was calculated by integrating the *ISO*/*SWS* spectrum (Meeus et al. 2001). The color difference due to the scattering process was derived as

$$\Delta(K - H_2O) = (K - H_2O)_{sca} - (K - H_2O)_{source},$$

where $(K - H_2O)_{sca}$ and $(K - H_2O)_{source}$ are the color of the scattered light and that for the illuminating source, respectively. $\Delta(K - L')$ is also described in the same manner. The derived color differences ($\Delta(K - H_2O)$ and $\Delta(K - L')$) are summarized in Table 1. There is no significant color gradient over the regions A – C. Figure 4 shows the observed color differences and a comparison with the model predictions. This figure indicates that the observed colors cannot be reproduced with silicate

Table 1
Color Differences of the Disk-Scattered Light Relative to the Illuminating Source

	$\Delta(K - H_2O)$	$\Delta(K - L')$
Region A	-0.88 ± 0.79	0.50 ± 0.53
Region B	-1.01 ± 0.63	0.43 ± 0.53
Region C	-1.16 ± 0.68	0.40 ± 0.56

grains alone, while they are consistent within 1σ error bars with models of a mixture of silicate and ice grains of $\sim 1\ \mu$m in size under an abundance of ice described by Miyake & Nakagawa (1993) (the mass fraction of ice to silicate is 94/43). The grain size of $\sim 1\ \mu$m is in agreement with that estimated in the *H* and *K* bands (Fukagawa et al. 2006) and in MIR (Fujiwara et al. 2006), which suggests that icy grains in the disk surface also experience grain growth. In addition, the fractional mass abundance of ice relative to silicate is inferred to be more than $\sim 9.4/43$ (see Figure 4).

4. DISCUSSION

We have detected water ice grains *on the surface* of the outer ($r > 140$ AU) disk around HD 142527. Using the stellar parameter of $T_{\rm eff} = 6250$ K and $L_* = 15\,L_\odot$ (Acke & van den Ancker 2004), we derived the dust temperature of the (superheated) surface layer in the outer disk. On the other hand, we estimated the expected partial pressure of H_2O at the surface from the saturated vapor pressure curve. And we found that the dust temperature is well below that needed for water ice condensation (~ 120 K), which is consistent with the detection of ice in our observations. However, when the effect of photosputtering due to UV irradiation is considered (Grigorieva et al. 2007), water ice grains may be unable to survive, since the disk surface is subjected to direct UV irradiation from the central star. One possibility is that the surface where the NIR scattered light originates from may be deeper than the superheated surface layer, where UV radiation does not reach and the photosputtering of water ice grains may be insufficient. Another explanation is that the photosputtering is not as effective relative to recondensation, due to the abundant water vapor in protoplanetary disks. Furthermore, turbulence in the disk can supply icy grains to the surface from a deeper layer of the disk. Further analysis is required to examine the validity of the above possibilities.

Finally, our results successfully demonstrate that multi-waveband ($K/H_2O/L'$) imaging is useful to detect water ice grains in a (face-on) disk. The application of this method for other face-on disks will enhance our knowledge on the presence and spatial distribution of water ice in circumstellar disks.

We are grateful to all of the staff members of the Subaru Telescope for providing us the opportunities to perform these observations, and for their support. We also thank Mr. Fujiwara for his useful comments.

REFERENCES

Acke, B., & van den Ancker, M. E. 2004, A&A, 426, 151
Carr, J. S., & Najita, J. R. 2008, Science, 319, 1504
Davis, S. S. 2007, ApJ, 660, 1580
Encrenaz, T. 2008, ARA&A, 46, 57
Fujiwara, H., et al. 2006, ApJ, 644, L133
Fukagawa, M., Tamura, M., Itoh, Y., Kudo, T., Imaeda, Y., Oasa, Y., Hayashi, S. S., & Hayashi, M. 2006, ApJ, 636, L153
Grigorieva, A., Thébault, P., Artymowicz, P., & Brandeker, A. 2007, A&A, 475, 755
Hayashi, C., Nakazawa, K., & Nakagawa, Y. 1985, in Protostars and Planets II, ed. D. C. Black & M. S. Matthews (Tucson, AZ: Univ. Arizona Press), 1100
Henden, A. A. 2002, JAAVSO, 31, 11
Inoue, A. K., Honda, M., Nakamoto, T., & Oka, A. 2008, PASJ, 60, 557
Kobayashi, H., Watanabe, S.-I., Kimura, H., & Yamamoto, T. 2008, Icarus, 195, 871
Leggett, S. K., et al. 2003, MNRAS, 345, 144
Malfait, K., Bogaert, E., & Waelkens, C. 1998, A&A, 331, 211
Malfait, K., Waelkens, C., Bouwman, J., de Koter, A., & Waters, L. B. F. M. 1999, A&A, 345, 181
Meeus, G., Waters, L. B. F. M., Bouwman, J., van den Ancker, M. E., Waelkens, C., & Malfait, K. 2001, A&A, 365, 476
Miyake, K., & Nakagawa, Y. 1993, Icarus, 106, 20
Morbidelli, A., Chambers, J., Lunine, J. I., Petit, J. M., Robert, F., Valsecchi, G. B., & Cyr, K. E. 2000, Meteorit. Planet. Sci., 35, 1309
Ohashi, N. 2008, Ap&SS, 313, 101
Pontoppidan, K. M., Dullemond, C. P., van Dishoeck, E. F., Blake, G. A., Boogert, A. C. A., Evans, N. J., II, Kessler-Silacci, J. E., & Lahuis, F. 2005, ApJ, 622, 463
Salyk, C., Pontoppidan, K. M., Blake, G. A., Lahuis, F., van Dishoeck, E. F., & Evans, N. J., II. 2008, ApJ, 676, L49
Tamura, M., et al. 2000, Proc. SPIE, 4008, 1153
Terada, H., Tokunaga, A. T., Kobayashi, N., Takato, N., Hayano, Y., & Takami, H. 2007, ApJ, 667, 303
Tokunaga, A. T., & Vacca, W. D. 2005, PASP, 117, 421
Waelkens, C., et al. 1996, A&A, 315, L245
Whittet, D. C. B. (ed.) 2003, Dust in the Galactic Environment in Astronomy and Astrophysics (2nd ed., Bristol: Institute of Physics Publishing)